J. Micromech. Microeng. **10** (2000) 483–491. Printed in the UK PII: S0960-1317(00)08928-2

On the design of piezoresistive silicon cantilevers with stress concentration regions for scanning probe microscopy applications

R Bashir†‡‖, A Gupta†, G W Neudeck†, M McElfresh§ and R Gomez†

† School of Electrical and Computer Engineering, Purdue University, W Lafayette, IN 47907, USA
‡ Department of Biomedical Engineering, Purdue University, W Lafayette, IN 47907, USA
§ Department of Physics, Purdue University, W Lafayette, IN 47907, USA

E-mail: bashir@ecn.purdue.edu

Received 22 October 1999, in final form 23 May 2000

Abstract. In this paper, the design of silicon based cantilevers for scanning probe microscopy has been described in detail. ANSYS software has been used as a tool to design and model the mechanical properties of the silicon based cantilevers. The incorporation of stress concentration regions (SCRs) with a thickness smaller than the cantilever thickness, to localize stresses, has been explored in detail to enhance the piezoresistive displacement, force, and torque sensitivity. In addition, SCRs of widths less than the cantilever width have also been explored. Two basic designs were studied, i.e. a rectangular cantilever and a U-shaped cantilever. The placement of the SCR was found to be critical, and optimal placement and thickness of the SCR can result in a 2× and 5× improvement in piezoresistive displacement and force sensitivity, respectively, for the rectangular cantilever. For the U-shaped cantilever, the torsional piezoresistive sensitivity was found to increase by 5×, depending on the SCR thickness. Process flows and associated fabrication challenges for the proposed cantilever structures are also presented.

(Some figures in this article are in colour only in the electronic version; see www.iop.org)

1. Introduction

Silicon microelectromechanical systems (MEMS) technology has been used to produce a variety of systems-on-a-chip in the consumer, automotive, biomedical, and industrial market segments [1]. The key features of introducing silicon technology for these applications include: (i) a very high degree of control of dimensions; (ii) miniaturization of the devices and mechanical elements; and (iii) the possibility of batch fabrication and hence the subsequent reduction of cost from economies of scale. One of the areas where silicon MEMS technology is being used commercially is in the fabrication of cantilevers and probes for scanning probe microscopy (SPM) applications. SPM refers to a family of instruments used to measure the properties of surfaces in length scales that range from inter-atomic spacing to a tenth of a millimetre. Atomic force microscopy (AFM) and scanning tunnelling microscopy (STM) are specific examples of SPM. Since it was first reported in 1986 [2], AFM technology has progressed to the point that it is now commercially used in semiconductor research and manufacturing for surface roughness measurements, two-dimensional (2D) depth profiling, and critical dimension measurements [3–5], as well as a possible tool for non-standard lithography [6, 7]. Additionally, AFM technology has also been used for interrogating surface properties of biological materials [8, 9], and to study interactions between biological molecules [10].

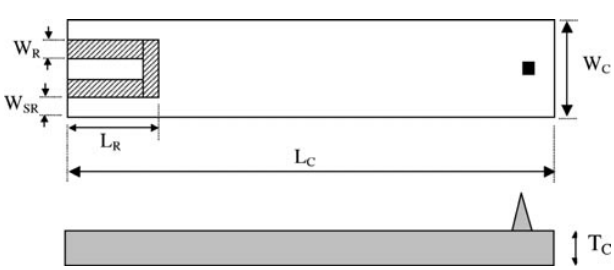

Figure 1. A schematic diagram of the rectangular cantilever used in the simulation study. The appropriate design dimensions are shown in table 1.

The key components of the atomic force microscope are a cantilever with an integrated tip and a deflection

‖ Author to whom correspondence should be addressed.

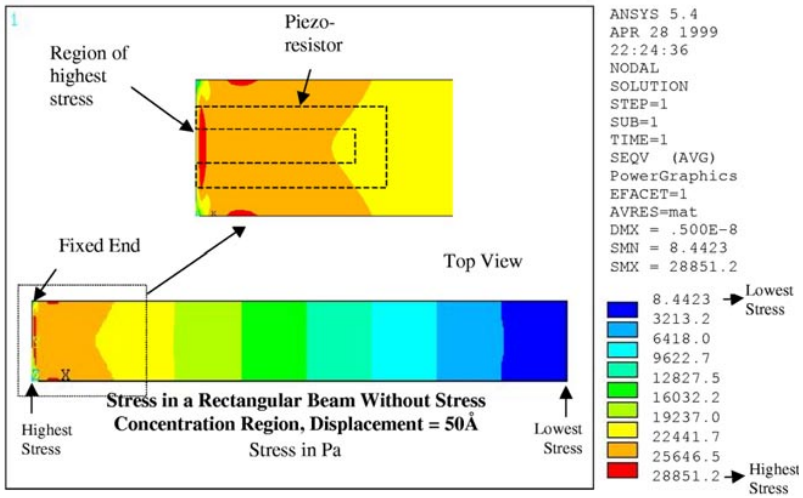

Figure 2. Top view 2D plot of the von-Mises stress contours, as obtained from ANSYS, for the rectangular beam.

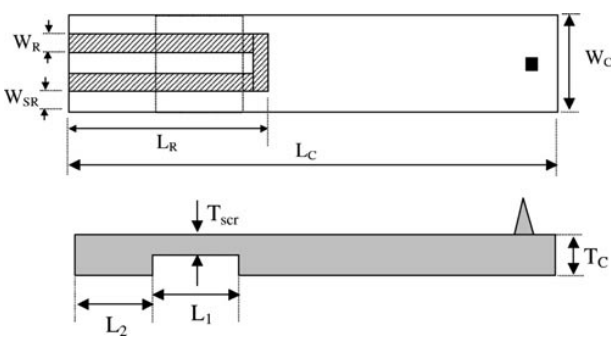

Figure 3. A schematic diagram of the rectangular cantilever used in the simulation study. The appropriate design dimensions, with the stress concentration regions, are listed in table 2.

Table 1. List of parameters and dimensions for the rectangular cantilever, as shown in figure 1.

Parameters and dimensions	
Piezoresistive properties	p-type $N_A = 10^{17}$ cm^{-3} $\langle 110 \rangle$ in (001) plane $\pi_L = 71.8 \times 10^{-11}$ Pa^{-1} $\pi_T = -66.3 \times 10^{-11}$ Pa^{-1}
Cantilever dimensions	$L_C = 150$ μm $W_C = 20$ μm $T_C = 0.6$ μm
Resistor dimensions	$W_R = 4$ μm $W_{SR} = 4$ μm $L_R = 14$ μm or 24 μm

Table 2. List of parameters and dimensions for the rectangular cantilever with SCR, as shown in figure 3.

Parameters and dimensions	
Cantilever dimensions	$L_C = 150$ μm $W_C = 20$ μm $T_C = 0.6$ μm
Resistor dimensions	$W_R = 4$ μm $W_{SR} = 4$ μm $L_R = 14$ μm or 24 μm
SCR dimensions	$L_1 = 10$ μm and $L_2 = 10$ μm $L_1 = 0$ μm and $L_2 = 10$ μm $L_1 = 0$ μm and $L_2 = 20$ μm $T_{scr} = 0.1$, 0.2, 0.3, 0.4 and 0.5 μm

sensing mechanism. The design of the cantilever requires the appropriate choice of dimensions, stiffness constant, and resonant frequency to satisfy certain measurement requirements. For simple rectangular cantilevers closed form expressions of these parameters have been derived. However, for more complex structures, finite element modelling is useful to analyse and optimize these structures [3]. In addition, the actual mechanism for detection of the cantilever deflections is also very important. Piezoresistive detection is very attractive due to the fact that it eliminates the use of lasers and complicated optics, and has the potential of multiple cantilever operation [5, 11–14]. The enhancement of force and displacement detection sensitivity is of great interest since smaller deflections can then be measured with greater accuracy. The enhancement in piezoresistive sensitivity using structural modifications has been briefly described earlier [15].

The purpose of this paper is to describe in detail the design of silicon-based cantilevers for SPM using finite element analysis (FEA) software, ANSYS [16]. Specifically, the piezoresistive sensitivity enhancement due to the use of novel stress concentration regions (SCRs), with thickness and width less than the rest of the cantilever, to localize stresses, is examined. Two basic designs were studied, i.e. a conventional rectangular cantilever and a U-shaped cantilever. The placement of the SCR was found to be critical, and optimal placement and thickness of the cantilever can result in increased piezoresistive displacement, force, and torque sensitivity for the cantilevers. Fabrication flows and challenges are also presented.

2. Cantilever design and methodology

The FEA software, ANSYS, was used for the mechanical design of the cantilevers, with the main focus being to

Table 3. List of simulated parameters for the rectangular cantilever, with and without the SCR regions of various designs.

Parameter	$L_R = 14\ \mu m$ $T_{scr} = 0\ \mu m$ (no SCR)	$L_R = 24\ \mu m$ $T_{scr} = 0.3\ \mu m$ $L_1 = 10\ \mu m$ $L_2 = 10\ \mu m$	$L_R = 24\ \mu m$ $T_{scr} = 0.3\ \mu m$ $L_1 = 20\ \mu m$ $L_2 = 0\ \mu m$	$L_R = 14\ \mu m$ $T_{scr} = 0.3\ \mu m$ $L_1 = 10\ \mu m$ $L_2 = 0\ \mu m$
$(\Delta R/R)/D$ (Å^{-1}) (vertical)	3.27×10^{-7}	4.87×10^{-7}	5.43×10^{-7}	7.54×10^{-7}
$(\Delta R/R)/F$ (nN^{-1}) (vertical)	7.76×10^{-5}	2.43×10^{-4}	4.33×10^{-4}	4.04×10^{-4}
k (N m^{-1})	4.22×10^{-2}	2.00×10^{-2}	1.25×10^{-2}	1.87×10^{-2}
f_0 (kHz)	32.35	21.064	16.127	19.836

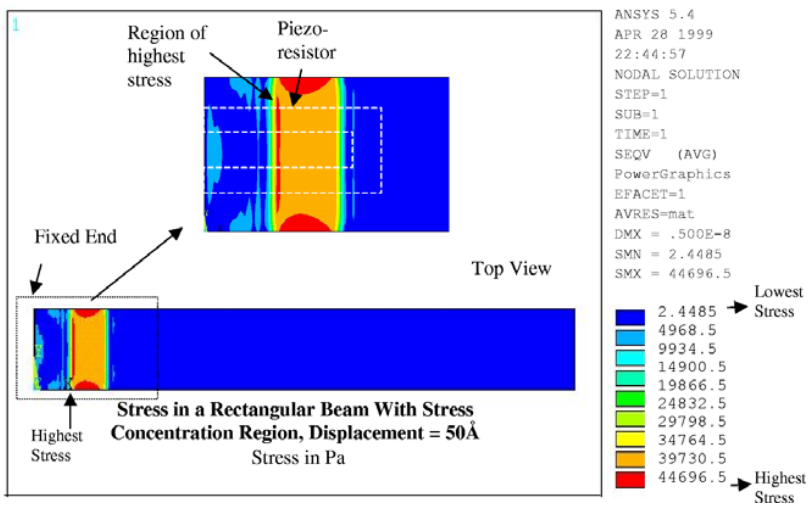

Figure 4. Top view 2D plot of the von-Mises stress contours, as obtained from ANSYS, for the rectangular beam with a stress concentration region. Clearly the stress is displaced and localized in the SCR region.

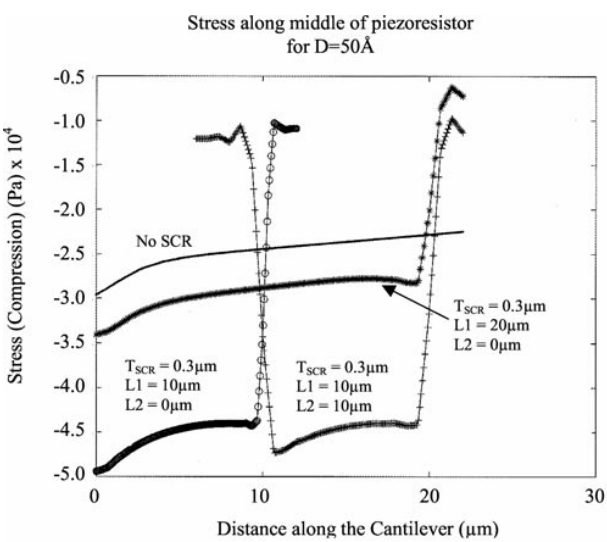

Figure 5. 1D stress plots along the resistor length of the four cantilever designs.

increase the piezoresistive deflection, force, and torque sensitivity. The piezoresistive effect in silicon results in a change in resistance R with applied stress, as a function of crystal orientation, dopant type, and doping concentration [17]. For a resistor with area A_R, the piezoresistive sensitivity is given by

$$\left.\frac{\Delta R}{R}\right|_{\substack{\text{Unit displacement,}\\ \text{Force, or Torsion}}} = \frac{1}{A_R}\int_0^{A_R} (\pi_L \sigma_L + \pi_T \sigma_T)\, \partial A \qquad (1)$$

where π_L is the longitudinal piezoresistive coefficient (for stress applied parallel to the current flow), π_T is the transverse piezoresistive coefficient (for stress applied perpendicular to the current flow in the resistor), σ_L is the longitudinal stress in the silicon, σ_T is the transverse stress in the silicon, and A_R is the area of the resistor. The piezoresistive deflection sensitivity is given by $\Delta R/R$ (change in resistance divided by total resistance) per unit of displacement and the piezoresistive force sensitivity is given by $\Delta R/R$ per unit of applied force. Thus, maximizing the stress in the resistor region will maximize the piezoresistive sensitivity of the device. Hence, the design methodology consisted of simulating the mechanical stresses in the silicon using ANSYS for a desired structure and then integrating that stress along the length of the resistor to obtain a numerical value of $\Delta R/R$ for a fixed applied displacement, force, or torque. For the case of the U-shaped cantilever, a torque is applied along the centre of the cantilever and the piezoresistive vertical displacement and force sensitivity are also obtained.

The analysis performed here uses the stress at the surface of the cantilever only and the effects of the depth of the piezoresistive sensing regions are ignored for simplification.

Table 4. List of simulated parameters for the U-shaped cantilever, with and without the SCR regions of various designs.

Parameter	$L_R = 14\ \mu m$ $T_{scr} = 0\ \mu m$ (no SCR)	$L_R = 24\ \mu m$ $T_{scr} = 0.3\ \mu m$ $L_1 = 10\ \mu m$ $L_2 = 10\ \mu m$	$L_R = 24\ \mu m$ $T_{scr} = 0.3\ \mu m$ $L_1 = 20\ \mu m$ $L_2 = 0\ \mu m$	$L_R = 14\ \mu m$ $T_{scr} = 0.3\ \mu m$ $L_1 = 10\ \mu m$ $L_2 = 0\ \mu m$
$(\Delta R/R)/D$ (Å^{-1}) (vertical)	3.34×10^{-7}	5.08×10^{-7}	5.57×10^{-7}	7.72×10^{-7}
$(\Delta R/R)/F$ (nN^{-1}) (vertical)	3.88×10^{-5}	1.25×10^{-4}	2.21×10^{-4}	2.02×10^{-4}
$(\Delta R/R)/\tau$ (pN m^{-1}) (torsional)	1.37×10^{-4}	2.32×10^{-4}	3.2×10^{-4}	3.4×10^{-4}
k (N m^{-1})	8.6×10^{-2}	4.05×10^{-2}	2.52×10^{-2}	3.82×10^{-2}
f_0 (kHz)	37.49	22.48	17.16	20.71

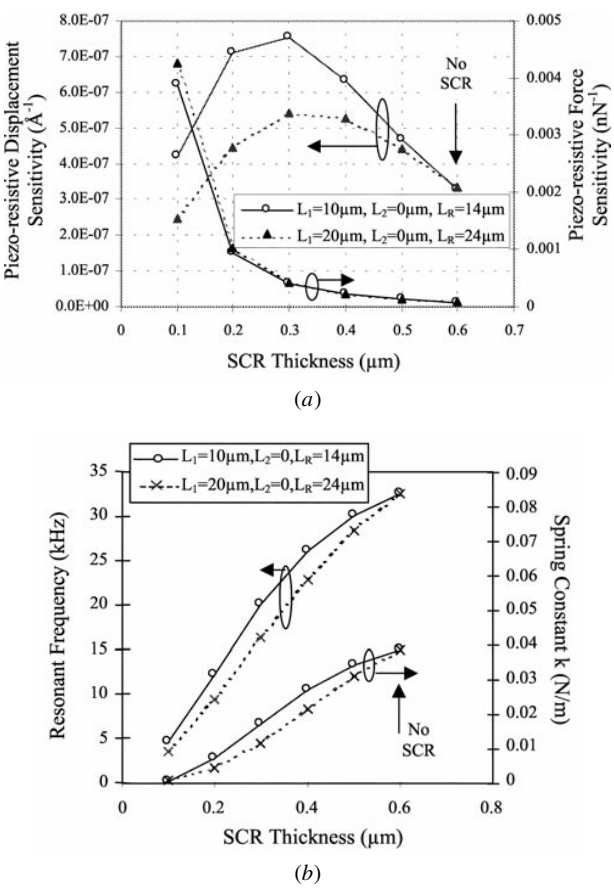

Figure 6. (*a*) Piezoresistive displacement and force sensitivity as a function of SCR thickness. (*b*) Resonant frequency and spring constant as a function of SCR thickness. $L_2 = 0$ for these results, i.e. the SCR is placed next to the cantilever edge.

In typical cantilevers, the piezoresistive regions will have a finite depth that is less than the cantilever thickness. There have been recent reports of 0.1 μm thick cantilevers with resistors confined to the upper third of the thickness [18]. Hence, it is assumed that there will be fabrication processes developed to form resistors even in ultra thin (<100 nm) cantilevers. The process flow section in this paper also proposes novel techniques to form such resistors.

For the ANSYS simulations described in this paper, Young's modulus of 1.3×10^{11} N m^{-2}, Poisson's ratio of 0.279 and density of silicon of 2.27×10^3 kg m^{-3} were

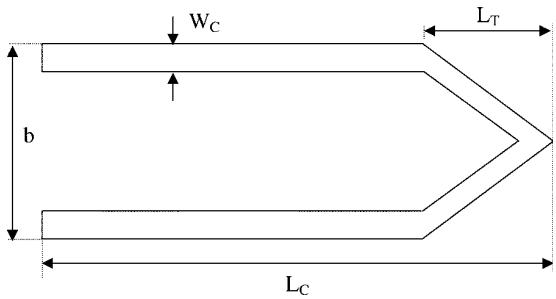

Figure 7. A schematic diagram of the U-shaped cantilever. The appropriate design dimensions are listed here. Piezoresistive properties: p-type $N_A = 10^{17}$ cm^{-3}; ⟨110⟩ in the (001) plane; $\pi_L = 71.8 \times 10^{-11}$ Pa^{-1}; $\pi_T = -66.3 \times 10^{-11}$ Pa^{-1}. Cantilever dimensions: $L_C = 150\ \mu$m; $W_C = 20\ \mu$m; $T_C = 0.6\ \mu$m; $L_T = 40\ \mu$m; $b = 80\ \mu$m. Resistor dimensions and SCR dimensions are the same as in figure 3.

used. Static analysis was used with element type SOLID5 to calculate the displacement and force sensitivity values. In order to obtain the resonant frequency, modal analysis was used with element type SOLID5. Static analysis was used with element type SOLID73 to calculate the torsional sensitivity for the U-shaped beam. All the loads were applied right at the edge of the structure. The mesh was increased in the regions where the piezoresistors would be implanted, as compared to the rest of the cantilevers, in order to capture the changes in stresses in the regions of importance.

2.1. Stress localization by reduced thickness for a rectangular cantilever

Figure 1 shows a schematic diagram of the cantilever and the relevant design dimensions. The piezoresistive properties and the dimensions of the resistor are shown in the inset in figure 1. Figure 2 shows the top view 2D plot of the von-Mises stress contours as obtained from ANSYS. The maximum stress occurs at the anchored edge as expected, and an integration of the stress using equation (1) can be used to determine a numerical value of the piezoresistive sensitivity. For a given unit deflection or displacement in the cantilever, the stress can be localized in a small region by adding SCRs which are thinner than the rest of the cantilever. In other words, the stress from the rest of the cantilever region is being displaced and concentrated within the SCRs. Placing the resistors over the SCRs increases the piezoresistive sensitivity

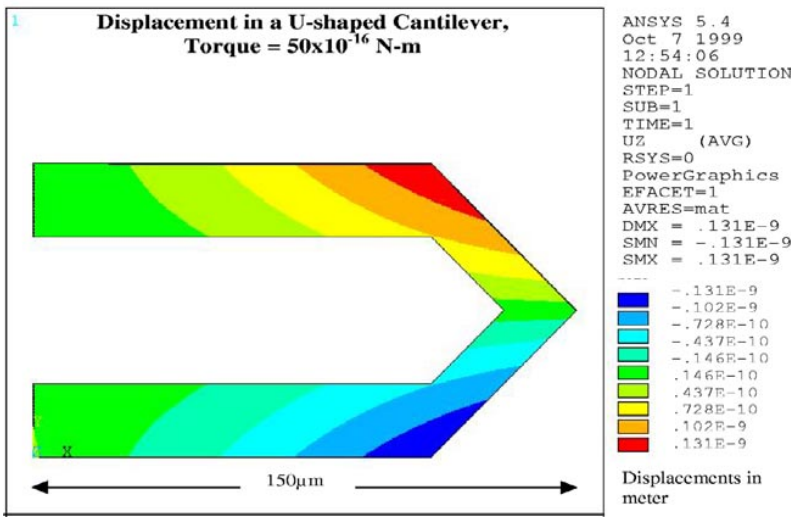

Figure 8. ANSYS top view plot of vertical displacement in the U-shaped cantilever with an applied torque of 50×10^{-16} N m^{-1}.

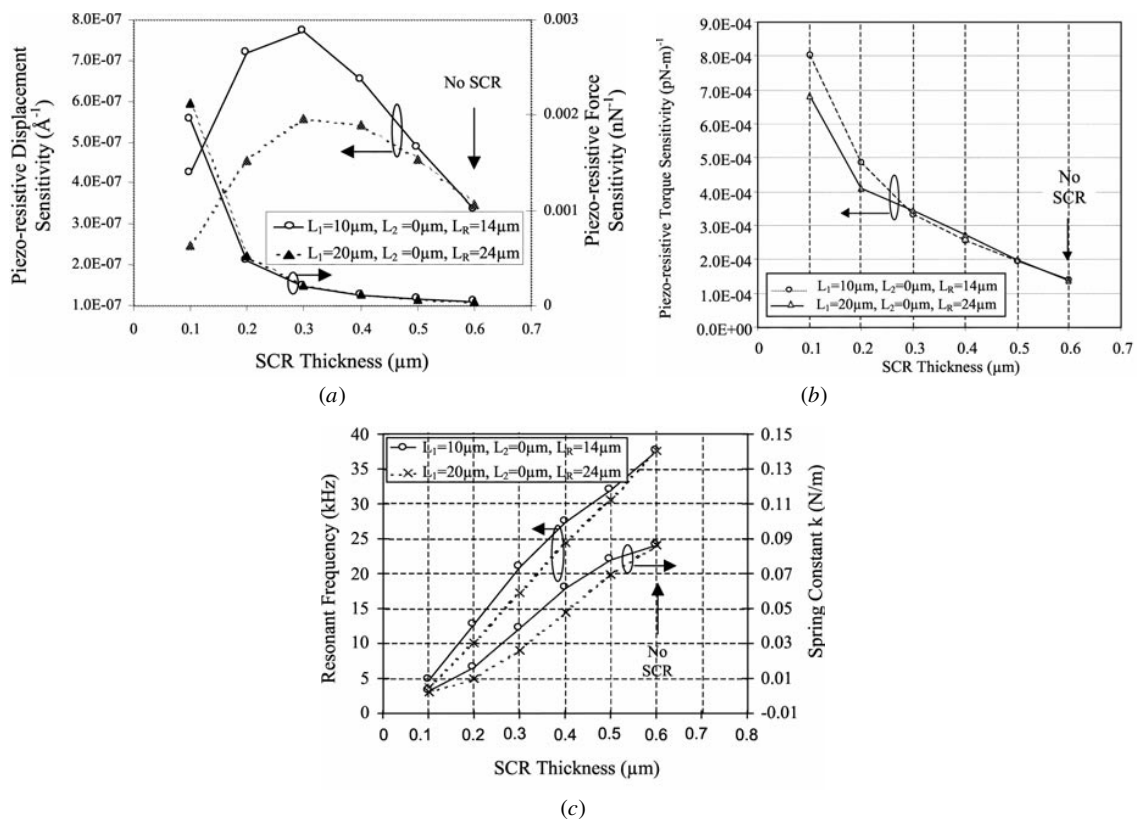

Figure 9. (*a*) Piezoresistive vertical displacement and force sensitivity as a function of SCR thickness. (*b*) Piezoresistive torsional sensitivity as a function of SCR thickness. (*c*) Resonant frequency and spring constant as a function of SCR thickness.

as dictated by equation (1). The location and thickness of these SCRs is also very important and two possible designs have been explored, as shown in figure 3. In one case, the SCR of length L_1 is placed a distance L_2 away from the edge. In the other case, $L_2 = 0$ and the SCR is placed right at the edge of the cantilever. SCR lengths (L_1) of 10 and 20 μm were simulated. In addition, the thickness of the SCR was also varied from 0.1 to 0.6 μm (0.6 μm thick SCR is the same as no SCR). Figure 4 depicts the top view stress contours clearly illustrating the concentration of stress within the SCR with a thickness of 0.2 μm. Table 3 shows the values of the various simulated mechanical parameters of a rectangular cantilever including the piezoresistive displacement and force sensitivity.

As can be noted from table 3, the piezoresistive sensitivity is enhanced, when compared to the case of no SCR, only under the appropriate choice of SCR width and thickness. When the SCR region is placed 10 μm away from the edge no enhancement is observed even though the stress is concentrated in the SCR region, as shown in figure 4.

Table 5. List of simulated parameters for the U-shaped cantilever, with and without the SCR regions of reduced width of two different designs (shown in figures 10 and 11).

Parameter	$L_R = 14\ \mu m$ $T_{scr} = 0\ \mu m$ (no SCR)	$L_R = 14\ \mu m$ $L_{scr} = 10\ \mu m$ $W_{scr} = 12\ \mu m$ $T_{scr} = 0\ \mu m$ (without gap)	$L_R = 14\ \mu m$ $L_{scr} = 10\ \mu m$ $W_{scr} = 4\ \mu m$ $T_{scr} = 0\ \mu m$ (with gap)
$(\Delta R/R)/D$ ($Å^{-1}$) (vertical)	3.34×10^{-7}	6.04×10^{-7}	9.79×10^{-7}
$(\Delta R/R)/F$ (nN^{-1}) (vertical)	3.88×10^{-5}	8.34×10^{-5}	1.55×10^{-4}
$(\Delta R/R)/\tau$ (pN m^{-1}) (torsional)	1.37×10^{-4}	2.70×10^{-4}	4.45×10^{-4}
k (N m^{-1})	8.6×10^{-2}	7.24×10^{-2}	6.32×10^{-2}
f_0 (kHz)	37.49	33.82	30.93

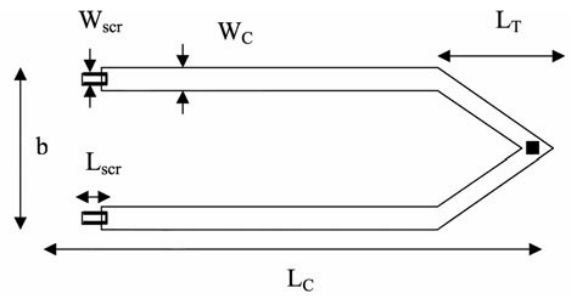

Figure 10. A schematic diagram of the U-shaped cantilever with reduced width used in the simulation study. The design dimensions and simulated parameters are listed here and are also listed in table 5. Piezoresistive properties: p-type $N_A = 10^{17}$ cm^{-3}; ⟨110⟩ in the (001) plane; $\pi_L = 71.8 \times 10^{-11}$ Pa^{-1}; $\pi_T = -66.3 \times 10^{-11}$ Pa^{-1}. Cantilever dimensions: $L_C = 150\ \mu m$; $W_C = 20\ \mu m$; $T_C = 0.6\ \mu m$; $L_T = 40\ \mu m$; $b = 80\ \mu m$. Resistor dimensions: $L_R = 14\ \mu m$; $W_R = 4\ \mu m$. SCR dimensions: $L_{scr} = 10\ \mu m$; $W_{scr} = 12\ \mu m$.

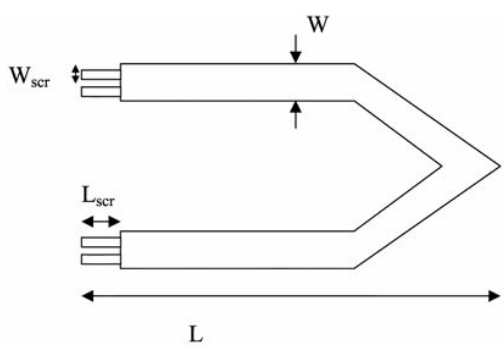

Figure 11. A schematic diagram of the U-shaped cantilever with reduced width and a gap between the resistors used in the simulation study. The design dimensions and simulated parameters are listed here and are also listed in table 5. Piezoresistive properties: p-type $N_A = 10^{17}$ cm^{-3}; ⟨110⟩ in the (001) plane; $\pi_L = 71.8 \times 10^{-11}$ Pa^{-1}; $\pi_T = -66.3 \times 10^{-11}$ Pa^{-1}. Cantilever dimensions: $L_C = 150\ \mu m$; $W_C = 20\ \mu m$; $T_C = 0.6\ \mu m$; $L_T = 40\ \mu m$; $b = 80\ \mu m$. Resistor dimensions: $L_R = 14\ \mu m$; $W_R = 4\ \mu m$. SCR dimensions: $L_{scr} = 10\ \mu m$; $W_{scr} = 4\ \mu m$.

Enhancement in piezoresistive sensitivity is observed only when the SCR is placed right next to the edge of the cantilever. This phenomenon is easily explained if the 1D plots of the stress contours in figure 5 are examined. Clearly, for the case of $L_2 = 10\ \mu m$, the integrated stress that comes into play is about the same as the integrated stress for the case of no SCR. To maximize the enhancement of the integrated stress (i.e. area under the curve) when compared to the case of no SCR, the SCR needs to be placed at the edge. The piezoresistive sensitivity was also found to be a function of the SCR thickness as shown in figure 6. The sensitivity can increase by a factor of two when the SCR thickness is decreased from 0.6 μm (the case of no SCR) to 0.3 μm, below which the sensitivity starts to decrease again. This phenomenon can be explained by the fact that the integrated stress along the given resistor length peaks around an SCR thickness of 0.3 μm. As the SCR thickness is decreased further, the spring constant of the cantilever also decreases, as shown in figure 6(*b*), and hence the total strain energy stored in the cantilever for a given displacement ($E = 1/2kx^2$) also decreases. Below about 0.3 μm, the total energy decreases significantly and so does the displacement sensitivity. On the other hand, the force sensitivity continues to increase with the decreasing SCR region and this is consistent with the fact that a thinner and longer (i.e. low k) cantilever is more sensitive to force and a thicker and shorter cantilever is more sensitive to displacement. Thus, using this approach of adding the SCR regions, cantilevers can potentially be used for simultaneous displacement and force sensitive measurements.

2.2. Stress localization by reduced thickness for a U-shaped cantilever

The U-shaped SPM design has been used for applications such as torque magnetometry [12] and lateral force microscopy [15]. Figure 7 shows the schematic diagram for such a cantilever design. In this case, a piezoresistor is placed on each leg of the cantilever and the torsion can be extracted by measuring $\Delta(R_1 - R_2)/(R_1 + R_2)$ per unit of applied torque and the vertical displacement by measuring $\Delta(R_1 + R_2)/(R_1 + R_2)$ per unit of applied displacement. If the resistors are assumed to be of the same value as they usually would be, the above sensitivity would simply be $\Delta R/R$, under the resultant stress in each leg of the cantilever. Figure 8 shows the simulated symmetrical displacement in the z-direction under an applied torque of 50×10^{-16} N m^{-1}. As expected, the stress is symmetric along the middle of the

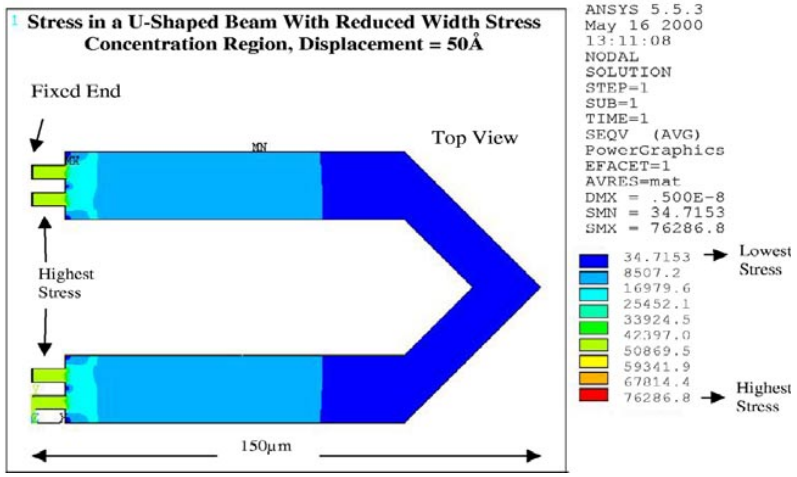

Figure 12. Top view 2D plot of the von-Mises stress contours, as obtained from ANSYS, for the U-shaped beam with reduced width stress concentration region.

cantilever and the top surface of one arm is under tension while the top surface of the other arm is under compression.

Table 4 shows the values of the various mechanical parameters for the U-shaped cantilever including the piezoresistive vertical displacement, force, and torsional sensitivity. As can be noted from table 4, and similar to the rectangular cantilever, the piezoresistive sensitivity is enhanced when compared to the case of no SCR only under the appropriate choice of the SCR width and thickness. The sensitivities are again enhanced only when the SCR region is placed right next to the anchored edge of the cantilever. The SCR displaces the stresses to the thinner regions and the corresponding displacement and force sensitivities are enhanced by a factor of 2.3× and 5×, respectively, without much decrease in the resonant frequencies. Figure 9(a) shows the sensitivities as a function of the SCR thickness for the U-shaped cantilever. The displacement sensitivity shows a similar trend as in the rectangular cantilever case, where the sensitivity maximizes at an SCR thickness of 0.3 μm. The vertical force sensitivity increases as the SCR thickness is decreased. Since torque is a rotational force measurement, the sensitivity also increases monotonically as the SCR thickness is decreased. The SCR design, as described here, can thus be used to obtain a simultaneous increase in force, displacement and torsional sensitivity for a variety of SPM applications.

2.3. Stress localization by reduced width for a U-shaped cantilever

An alternative approach to concentrating stress in the scanning probe cantilevers is to reduce the width of the cantilever in the region where the piezoresistor is to be placed. It should be mentioned that this approach is valid only when the width is not already at a minimum and can be reduced further. In that case, such an approach might be more amenable to processing since the width can be reduced by masking and etching processes rather than other schemes. Figure 10 shows the schematic layout of a scheme where the cantilever width is reduced close to the anchored edge. The resistors are placed in these regions of reduced width. Figure 11 shows the schematic layout of a scheme where the cantilever width is reduced and there is also a gap added between the regions where the resistor would be placed. Table 5 shows the simulated parameters and compares the case of no SCR, and the two SCR approaches mentioned above. Figure 12 shows the top view 2D plot of the von-Mises stress contours, as obtained from ANSYS, with a displacement of 50 Å applied to the edge. The stress is clearly concentrated in the SCR and the corresponding sensitivities are all enhanced by a factor of 1.5–2× for the layout without the gap and a factor of ∼3.5× for the layout with the gap between the resistor legs. Hence, the reduced width SCRs also provide another way to enhance the force, displacement, and torsional sensitivity of scanning probe cantilevers.

2.4. Process flows

The fabrication of ultra thin cantilevers is ideally suited using silicon-on-insulator (SOI) technology [19]. The structure with reduced thickness for the SCR can be fabricated using selective epitaxial growth (SEG) of silicon and chemical–mechanical polishing [20]. Figures 13(a)–(g) show the process sequence for such a process where SEG is ideally suited for fabricating these structures since the silicon can be grown over topography and steps, that are created within the underlying oxide film. Figure 14 shows a cross-section along the width of such a cantilever. This process can also be used to make thin cantilevers without the SCR since chemical–mechanical polishing has been shown to polish selective silicon overgrowths down to 150 nm [21]. The selective epitaxial silicon seed region acts as the natural anchor to the substrate and the thickness of the silicon cantilever is determined by the field oxide thickness and the chemical–mechanical polishing step. Such a process can also be envisioned through the use of SIMOX (simultaneous implantation of oxygen) or BESOI (bonded etched back SOI) wafers as the starting material [19] and SEG where the SEG is used to produce the anchor to the substrate. The buried oxide in these SOI wafers provides an etch stop while etching the silicon and the cantilever thickness is determined by the initial SOI film thickness. The tip in either process option

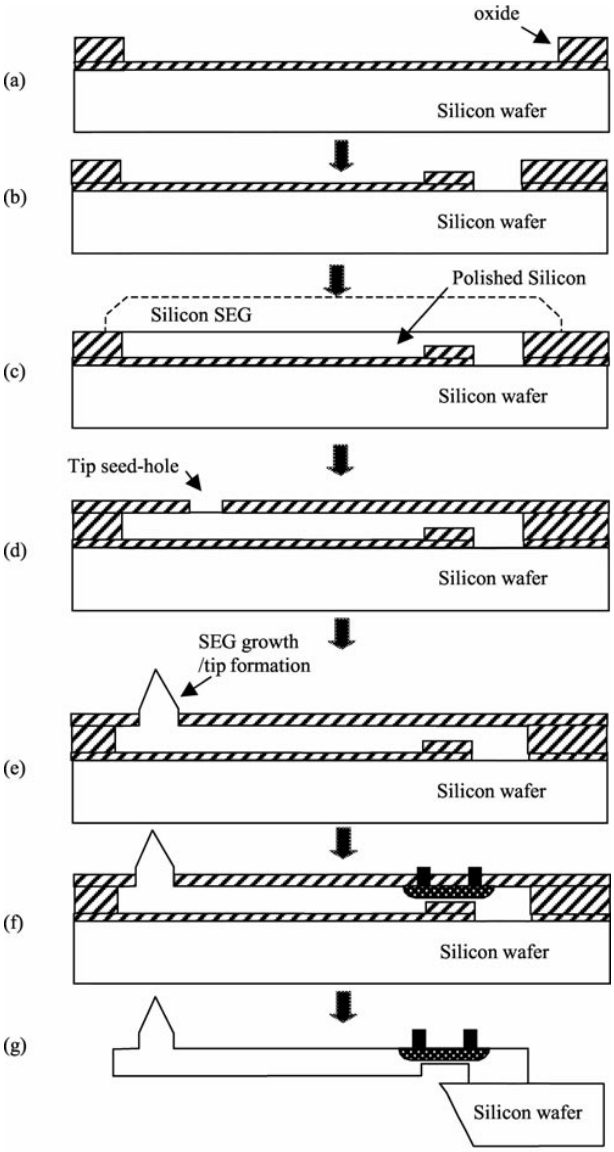

Figure 13. (*a*)–(*g*) Process flow for the proposed cantilevers using selective epitaxial growth (SEG) of silicon and chemical mechanical polishing showing the reduced thickness cantilever. The drawing is not to scale.

can be grown using selective epitaxial growth of silicon providing a very unique and novel way to form the tip without perturbing the cantilever. In addition, using this proposed process the cantilever and tip are formed independently, which is a significant advantage over SOI approaches, where the final cantilever thickness is achieved after the tip is etched and hence the two are not independently controlled. The piezoresistors can also be formed by selectively growing a thin silicon resistor using an oxide as a mask. Low-temperature selective growth has been shown to grow silicon (and related alloys) with a thickness down to 100 Å at temperatures as low as 625 °C using reduced pressure CVD growth techniques [22–23]. These proposed approaches and technologies are currently being pursued to verify the simulation results.

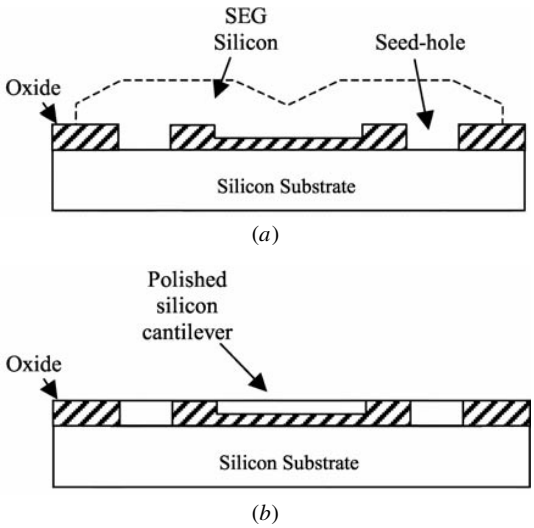

Figure 14. A cross-section (perpendicular to the one shown in figure 12(*c*)) of the structure showing the seed-hole, overgrowth, and polished cantilever regions.

3. Conclusions

In this paper, the design of silicon based cantilevers for SPM has been described in detail. The ANSYS software package was used as the basis to simulate the mechanical properties of the silicon based cantilevers. The incorporation of SCRs with a thickness less than the cantilever thickness, to localize stresses and thus enhance the piezoresistive displacement and force sensitivities, was explored in detail. In addition, the design of cantilevers of reduced width was also explored. Two basic designs were studied, i.e. a rectangular cantilever and a U-shaped cantilever. The placement of the SCR was found to be critical and optimal placement and thickness of the cantilever can result in a significant improvement in piezoresistive displacement, force, and torque sensitivities. Novel processes have also been proposed to fabricate the simulated structures.

References

[1] For a good overview of silicon micromachining and related applications, see the special issue: 1998 *Proc. IEEE* **86** (8)
[2] Binning G, Quate C and Gerber Ch 1986 Atomic force microscope *Phys. Rev. Lett.* **56** 930
[3] Brugger J, Buser R A and de Rooij N F 1992 Silicon cantilevers and tips for scanning force microscopy *Sensors Actuators* A **34** 193
[4] Tortonese M 1997 Cantilevers and tips for atomic force microscopy *IEEE Eng. Med. Biol. Mag.* (March/April) 28–33
[5] Indermuhle P F, Schurmann G, Racine G A and de Rooij N F 1997 Fabrication and characterization of cantilevers with integrated sharp tips and piezoelectric elements for actuation and detection for parallel AFM applications *Sensors Actuators* A **60** 186
[6] Minne S C, Soh H T, Flueckiger Ph and Quate C F 1995 *Appl. Phys. Lett.* **6** 703
[7] Minne S C, Flueckiger Ph, Soh H T and Quate C F 1995 Atomic force microscope lithography using amorphous silicon as a resist and advances in parallel operation *J. Vac. Soc. Technol.* B **13** 1380

[8] Hassan E A, Heinz W A, Antonik M D, D'Costa N P, Nageswaran S, Schoenenberger C and Hoh J H 1998 Relative microelastic mapping of living cells by atomic force microscopy *Biophys. J.* **74** 1564
[9] Lekka M, Lekki J, Marszalek M, Golonka P, Stachura Z, Cleff B and Hrynkiewicz A Z 1999 Local elastic properties of cells studied by SFM *Appl. Surf. Sci.* **141** 345
[10] Moy V T, Florin E and Gaub H 1994 Adhesive forces between ligand and receptor measured by AFM *Colloids Surf.* A **93** 343
[11] Su Y, Evans A G R, Brunnschweiler A, Ensell G and Koch M 1997 Fabrication of improved piezoresistive silicon cantilevers probes for the atomic force microscope *Sensors Actuators* A **60** 163
[12] Brugger J, Despont M, Rossel C, Rothuizen H, Vettiger P and Willemin M 1999 Microfabricated ultrasensitive piezoresistive cantilevers for torque magnetometry *Sensors Actuators* A **73** 235
[13] Gotszalk T, Radojewski J, Grabiec P B, Dumania P, Shi F, Hudek P and Rangelow I W 1998 Fabrication of multipurpose piezoresistive Wheatstone bridge cantilevers with conductive microtips for electrostatic and scanning capacitance microscopy *J. Vac. Sci. Technol.* B **16** 3948
[14] Jumpertz R, Hart A, Ohlsson O, Saurenbach F and Schelten J 1998 Piezoresistive sensors on AFM cantilevers with atomic resolution *Microelectron. Eng.* **41/42** 441
[15] Linneman R, Gotszalk T, Rangelow I W, Dumania P and Oesterschulze E 1996 Atomic force microscopy and lateral force microscopy using piezoresistive cantilever *J. Vac. Sci. Technol.* B **14** 856
[16] ANSYS is a product of Swanson Analysis Systems, Inc. `http://www.ansys.com/`
[17] Kovacs G 1998 *Micromachined Transducers Sourcebook* (New York: McGraw-Hill)
[18] Harley J A and Kenny T W 1999 High-sensitivity piezoresistive cantilevers under 1000 Å thick *Appl. Phys. Lett.* **75** 289
[19] Auberton-Herve A J 1996 SOI: materials to systems *Proc. 1996 IEDM* pp 3–10
[20] Bashir R, Neudeck G W, Yen H, Kvam E P and Denton J P 1995 Characterization of sidewall defects in selective epitaxial growth of silicon *J. Vac. Sci. Technol.* B **11** 923
[21] Neudeck G W, Pae S, Denton J P and Su T-C 1999 Multiple layers of silicon-on-insulator for nanostructure devices *J. Vac. Sci. Technol.* B **17** 994
[22] Bashir R, Kabir A E and Chao K 1999 Formation of self-assembled $Si_{1-x}Ge_x$ islands using reduced pressure chemical vapor deposition and subsequent thermal annealing of thin germanium rich films *Appl. Surf. Sci.* **152** 99
[23] Babcock J *et al* 2000 Precision electrical trimming of poly-SiGe resistors *IEEE Electron Device Lett.* **21** 283–5